



DAMAGE ASSESSMENT OF ECCENTRIC MULTISTOREY BUILDINGS USING 3-D PUSHOVER ANALYSIS

A.S. MOGHADAM and W.K. TSO

Department of Civil Engineering, McMaster University,
Hamilton, Ontario, L8S 4L7, Canada.

ABSTRACT

This paper presents a simplified procedure for the assessment of damage potential to eccentric multistorey buildings. A major assumption used is that the building will respond essentially in a single mode during the earthquake. The procedure uses the results of two 3-D pushover analyses together with the dynamic response of an equivalent single degree of freedom system to estimate the seismic deformation and damages of elements located at the perimeter of the building. The reliability of the procedure is demonstrated by applying it to assess the damages of a seven storey reinforced concrete eccentric frame building subjected to an ensemble of earthquake records of different characteristics.

KEYWORDS

Torsion, eccentricity, multistorey building, inelastic responses, pushover analysis, damage assessment.

INTRODUCTION

Excessive torsional responses in eccentric multistorey buildings have been a major cause of building damages in earthquakes (Esteve, 1987, Mitchell et al 1990). Torsional responses induce additional displacements on the flexible edge of the building. This results in additional ductility demands and drifts to elements (both structural and nonstructural) at or near this edge. Usually, a three-dimensional inelastic dynamic analysis of the complete building needs to be carried out in order to assess the damage potential of these elements. In this paper, a procedure is proposed to simplify the damage assessment process. The procedure is based on the equivalent single degree of freedom (SDOF) concept first proposed by Saiidi and Sozen (1981) to estimate the nonlinear seismic responses of structures. It involves the inelastic dynamic analysis of an SDOF system plus two inelastic analyses of the three-dimensional structure subjected to incremental static loading. This latter analysis will be referred to as a "3-D pushover analysis" for short.

PROCEDURE

The procedure is explained in detail for the case of an N-storey building having one axis of symmetry in the X direction. The building is subjected to ground motions perpendicular to the axis of symmetry and a damage assessment for the building is needed. The 2N equations of motion describing the deformation of the building can be expressed as:

$$\begin{bmatrix} M & 0 \\ 0 & I_m \end{bmatrix} \begin{Bmatrix} \ddot{\delta} \\ \ddot{\theta} \end{Bmatrix} + \{R\} = - \begin{bmatrix} M & 0 \\ 0 & I_m \end{bmatrix} \begin{Bmatrix} 1 \\ 0 \end{Bmatrix} \ddot{u}_g(t) \quad (1)$$

where $\{\delta\}$ is the Y-direction displacement vector referred to the centres of mass (CM) of the floors. $\{\theta\}$ is the floor rotation vector and $\{R\}$ is the restoring force vector. $[M]$ and $[I_m]$ are the mass matrix and mass moment of inertia matrix about CM, and $u_g(t)$ is the ground motion input. Assuming the building will respond to the ground excitation in a single mode, this MDOF system can be reduced to an equivalent SDOF system using the generalized coordinate approach as outlined by Collins(1995). Writing:

$$\begin{Bmatrix} \delta \\ \theta \end{Bmatrix} = \{\phi\} Y(t) \quad (2)$$

where $\{\phi\}$ represents an assumed constant deformation profile of the building and $Y(t)$ is the generalized coordinate. $\{\phi\}$ is normalized such that $Y(t)$ represents the CM displacement at the roof of the building. The deformation profile is obtained by means of a 3-D pushover analysis of the structure, applying a prescribed lateral force distribution $V\{f\}$ at the CMs of the building. V represents the base shear and $\{f\}$ the normalized distribution of the applied forces. During the pushover analysis, the base shear-roof CM deflection relationship is monitored. The resulting curve can be written as $V=K \times G(Y)$ where K is the initial slope of the V-Y curve and $G(Y)$ describes the bilinear approximation of the curve. Assuming the restoring force vector $\{R\}$ can be represented by the set of forces used in the pushover analysis, one can reduce the set of equations to a single equation, describing the motion of the equivalent SDOF system in the form:

$$M^* \ddot{Y} + K^* G(Y) = -L^* \ddot{u}_g(t) \quad (3)$$

where M^* , K^* and L^* denote the generalized mass, stiffness, and earthquake-excitation factor respectively for the equivalent SDOF system.

The solution of equation (3) is obtained using a step by step integration procedure and the absolute maximum of $Y(t)$, denoted by Y_{max} is a predictor of the maximum CM displacement at the roof of the structure. Once, Y_{max} is determined, a second 3-D pushover analysis will be carried out. The second pushover analysis terminates when the CM displacement at the roof of the structure equals to Y_{max} . The deformation and damage on elements near the flexible edge of the building at this stage of the pushover analysis would then be taken as indicative of the deformation and damage of these elements in the building when the building is subjected to the earthquake ground shaking.

EXAMPLE

A seismic damage assessment is performed on a uniform seven-storey reinforced concrete building to illustrate the procedure. The building has a rectangular plan measuring 24m by 17m. The lateral load resisting elements in the Y-direction consist of three identical ductile moment resisting frames. Frame 2 is located at the geometric centre of the plan and the spacing between frames is 9m, as shown in Fig.(1). Each frame has three bays and uniform storey height of 3 m. The building is designed for 0.3g effective peak acceleration, and the design spectrum has a shape similar to the Newmark-Hall 5% damped average spectrum. The base shear of the building is 1190 kN. Each frame is designed to take one third of the base shear. The strengths of the beams and columns in the frames are allocated following the "strong column-weak beam" capacity design procedure as outlined in the Canadian concrete design code. The building is eccentric due to uneven distribution of floor masses. The mass distribution of each floor causes the CM of the floor to shift 2.4m from frame 2 towards frame 3. Therefore, the building is mass eccentric and has a constant floor eccentricity equal to 10% of the plan dimension. The right hand edge is the flexible edge susceptible to large additional displacements, and frame 3 is the frame that is the most vulnerable in terms of ductility demands.

Thirteen earthquake records are used as ground motion inputs. The first seven records are mainly Californian records that have been used extensively by many researchers. Records 8 and 9 are the SCT records obtained in Mexico city during the 1985 Michanocan earthquake. Records 10 to 13 are four near field records obtained during the 1994 Northridge earthquake. These four records are included in this study as they have been shown to have different characteristics compared to the "El-Centro 1940" type of records, and can lead to very large drift in multistorey buildings (Iwan 1995). Records of different characteristics are chosen in order to check out the proposed procedure under a wide variety of seismic environments. Details of the records can be found in Table (1).

To initiate the procedure, a triangular load distribution is used for the 3-D pushover analysis. The resulting base shear-roof CM deflection relation is obtained and approximated as a bilinear curve for the $G(Y)$ function of the equivalent SDOF system. To allow for unloading to take place, the $G(Y)$ function is assumed to be bilinear hysteretic. Following the suggestion of Qi and Moehle (1991), the deformation profile when the top CM displacement equals to 1% of the total height is taken to create the equivalent SDOF system. For each earthquake record, a dynamic analysis on the SDOF system is performed to obtain the Y_{max} . Another 3-D pushover analysis is then carried out to determine the state of stress and deformation of the building at the flexible edge and also at frame 3, when the CM displacement at the roof of the building reaches Y_{max} . These quantities are compared with those obtained using a three dimensional inelastic dynamic analysis of the building. The CANNY computer code (Li, 1993) is used to carry out the analyses. In all dynamic analyses, 5% viscous damping is incorporated in the computation.

RESULTS

The base shear-roof CM deflection relation is shown in Fig. (2). This curve is approximated as a bilinear curve with the effective yield displacement at 0.075m. The displacement profiles at four stages of loading are presented in Fig.(3). These four stages correspond to the roof CM deflection equals to one times, two times, three times and four times the effective yield displacement respectively. Fig.(3a) shows the displacement profile at the CM of the floors, while the corresponding displacement profiles at the flexible edge are shown in Fig. (3b). The difference of the profiles in Figs. (3a, 3b) is a result of the rotational deformation of the floors. The interstorey drift ratio profiles at these four stages of loading are shown in Figs.(4a, 4b). A comparison of the curves in this figure shows that due to torsion, the interstorey drift ratio at the flexible edge is about 1.7 times those at CM.

Fig. (5) compares the maximum roof displacement at CM, using the proposed procedure and the MDOF dynamic analysis. Each point is generated by one earthquake record input. Two sets of symbols are used to segregate the results using the first nine earthquake records in Table (1), and the four Northridge records. Overall, the correlation between the two approaches is good.

The comparison of the deformation at the flexible edge are shown in Figs. (6 and 7). The maximum top displacement comparison is given in Fig.(6) and the maximum interstorey drift ratio in Fig.(7). The correlation is good, except for the cases where the near field Northridge earthquake records are used. The damage indices, as represented by the maximum ductility demand in the beams and columns of frame 3, are also compared and presented in Figs.(8 and 9).The correlation is not as good as the maximum deformation parameters. Results based on two of the near field Northridge earthquake records show that the proposed procedure can lead to large underestimation of beam and column ductilities in frame 3.

The next step of comparison is on the distribution of parameters of interest along the height of the building. Shown in Figs. (10a, 10b) are the maximum floor displacement and interstorey drift ratio distributions at the flexible edge. The Whittier earthquake record is used as input for the computation because it has provided a good correlation on the overall deformation and damage parameters as shown by the "solid square" points in figures 6 to 9. Shown in Figs. (11a, 11b) are the comparison on the beam ductility and column ductility distributions. The correlations for all four distributions are good. Figures (10) and (11) demonstrate that if the overall

deformation and damage parameters are well correlated, one can expect their distribution will also be well correlated.

CONCLUSIONS

A procedure to assess the seismic deformation and damage of eccentric multistorey buildings is proposed. This procedure combines the results of two 3-D pushover analyses together with the dynamic response of an equivalent SDOF system to estimate the seismic deformation and damages experienced by the building. Applying the procedure to a seven storey reinforced concrete eccentric building, it is shown that the procedure can generally lead to a good estimation of the seismic damage at the critical edge and the critical frame of the building over a variety of ground motions. The exception is for the class of near field ground motions as exemplified by the four Northridge earthquake records where the procedure may underestimate the damage. Considering the simplification in computation, the proposed procedure appears to be a promising approach for damage assessment of eccentric multistorey buildings.

ACKNOWLEDGMENT

The first author wishes to thank the Ministry of Culture and Higher Education of Iran for his scholarship. The support of the Natural Sciences and Engineering Research Council of Canada (NSERC) on the work reported herein is gratefully acknowledged.

REFERENCES

- Collins, K.R. (1995). A reliability-based dual level seismic design procedure for building structures. *Earthquake Spectra*, **11**, 417-429.
- Esteve, L. (1987). Earthquake engineering research and practice in Mexico after 1985 Earthquake. *Bull. N.Z. Natl. Soc. Earthquake Eng.*, **20**, 159-200.
- Iwan, W.D. (1995). Near-field considerations in specification of seismic design motions for structures. *Proc. 10th European Conf. on Earthquake Eng.*, Vienna, Austria, **1**, 257-267.
- Li, K-N. (1993). CANNY-C: A computer program for 3D nonlinear dynamic analysis of building structures. *Research report No. CE004*, National University of Singapore.
- Mitchell, D. et al., (1990). Damage to buildings due to the 1989 Loma Prieta earthquake--a Canadian code perspective. *Can. J. Civil Eng.* **17**, 813-834.
- Qi, X. and J.P. Moehle. (1991). Displacement design approach for reinforced concrete structures subjected to earthquakes. *Report UCB/EERC-91/02*, Earthquake Engineering Research Centre, University of California-Berkeley.
- Saidii, M. and M. Sozen. (1981). Simple nonlinear seismic analysis of R/C structures. *J. Struct. Div., ASCE*, **107**, 937-952.

Table 1. The earthquake records

Record No.	Earthquake	Magnitude	Epicentre Distance (km)	Component
1	Imperial Valley, 1940	6.6	8	S00E
2	Kern County, 1952	7.6	56	S69E
3	San Fernando, 1971, Lankershim Blvd.	6.4	24	S90W
4	San Fernando, 1971, 6th St., L.A.	6.4	39	S00W
5	Whittier, 1987, Griffith park	6.1	21.5	N0
6	Alaskan Subd. Zone, 1983	5.8	13	N270
7	Parkfield, 1966, Shandon No. 5	5.6	5	N85E
8	Mexico, 1985, SCT	8.1	375.5	N180
9	Mexico, 1985, SCT	8.1	375.5	N270
10	Northridge, 1994, Rinaldi	6.7	10	N-S
11	Northridge, 1994, Rinaldi	6.7	10	E-W
12	Northridge, 1994, Sylmar, Co. Hospital	6.7	16	N-S
13	Northridge, 1994, Sylmar, Co. Hospital	6.7	16	E-W

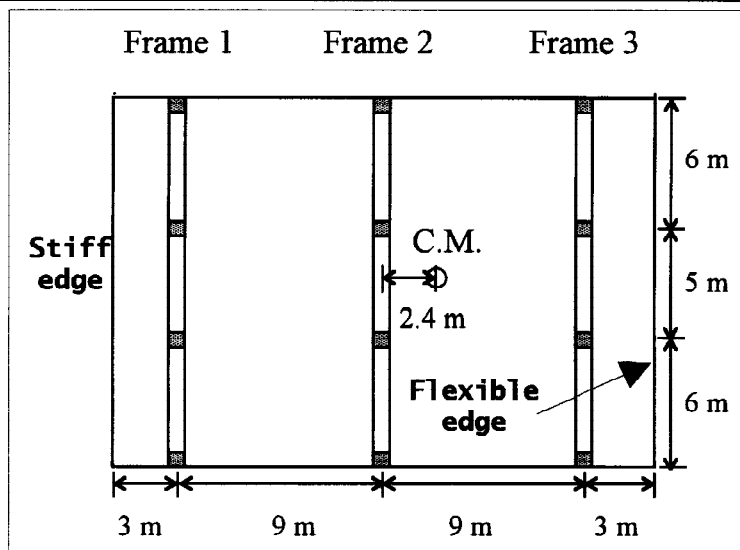


Fig. 1. Building Plan

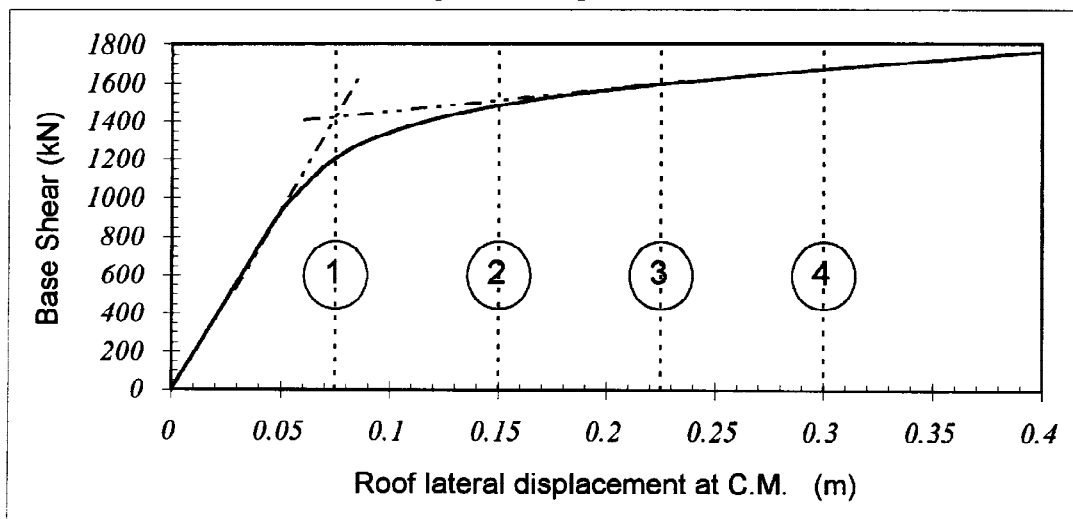


Fig. 2. Base shear-roof lateral displacement at C.M.

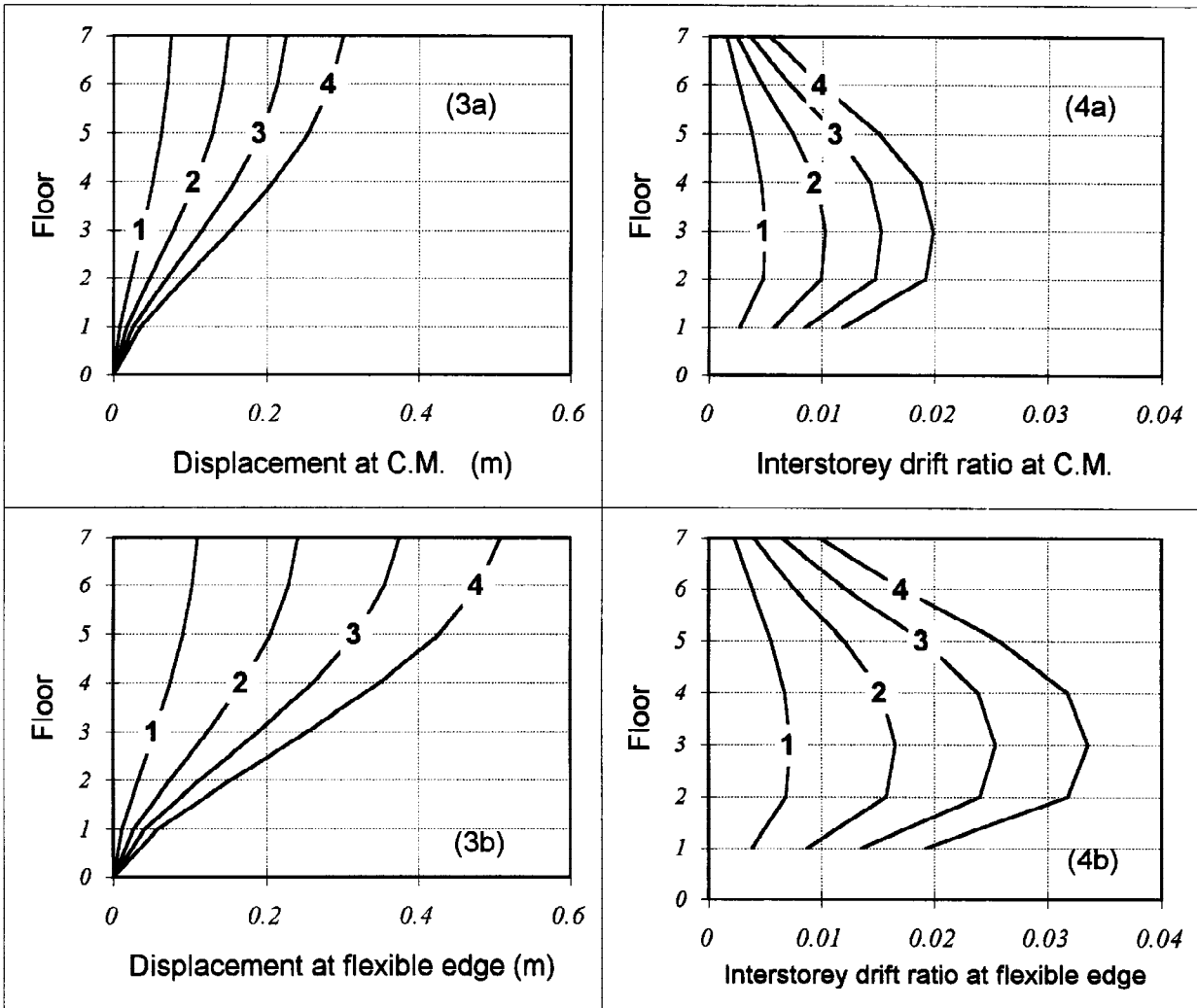


Fig. 3. Floor displacement profile (a) at C.M. , (b) at flexible edge

Fig. 4. Interstorey drift ratio (a) at C.M. , (b) at flexible edge

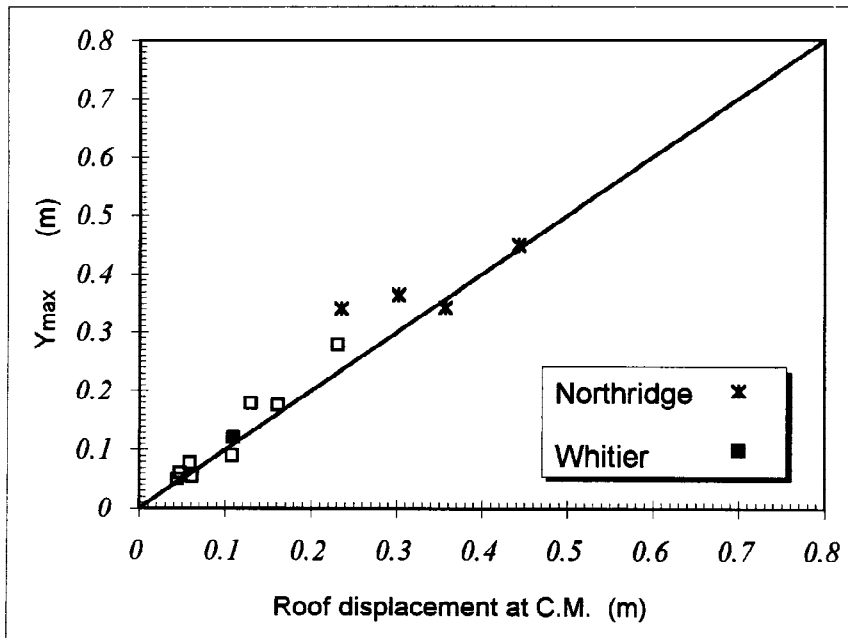


Fig. 5. Maximum displacement using SDOF and MDOF dynamic analyses

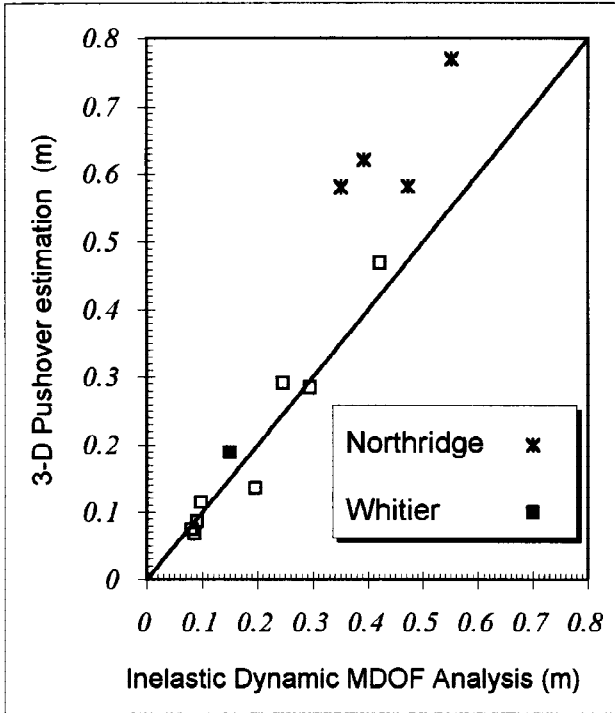


Fig. 6. Maximum top displacement at flexible edge

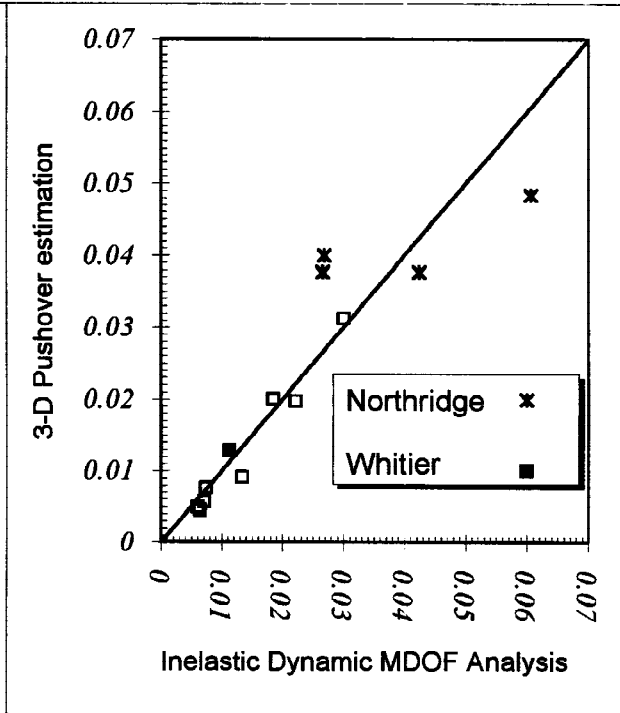


Fig. 7. Maximum interstorey drift ratio at flexible edge

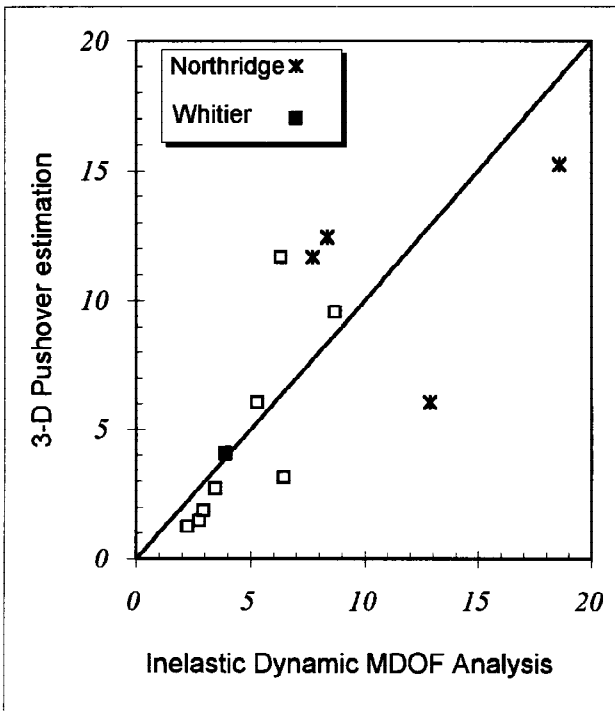


Fig. 8. Maximum ductility demand of beams on Frame 3

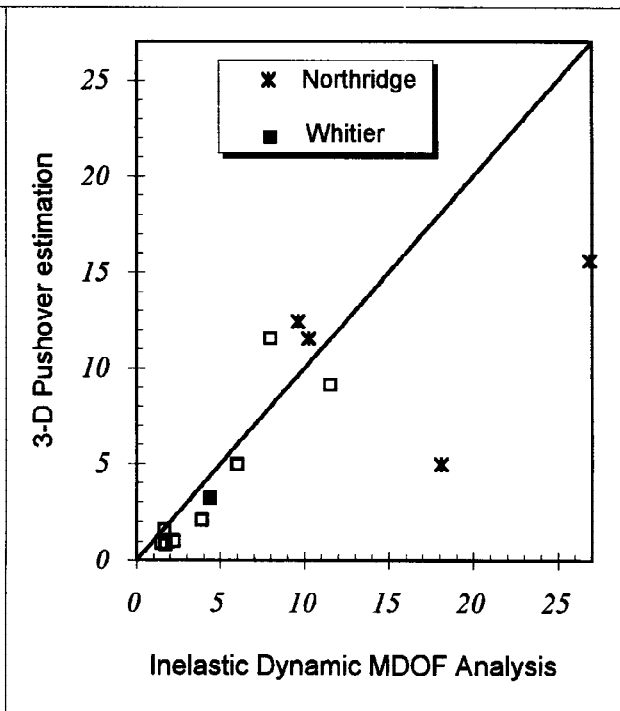


Fig. 9. Maximum ductility demand of columns on Frame 3

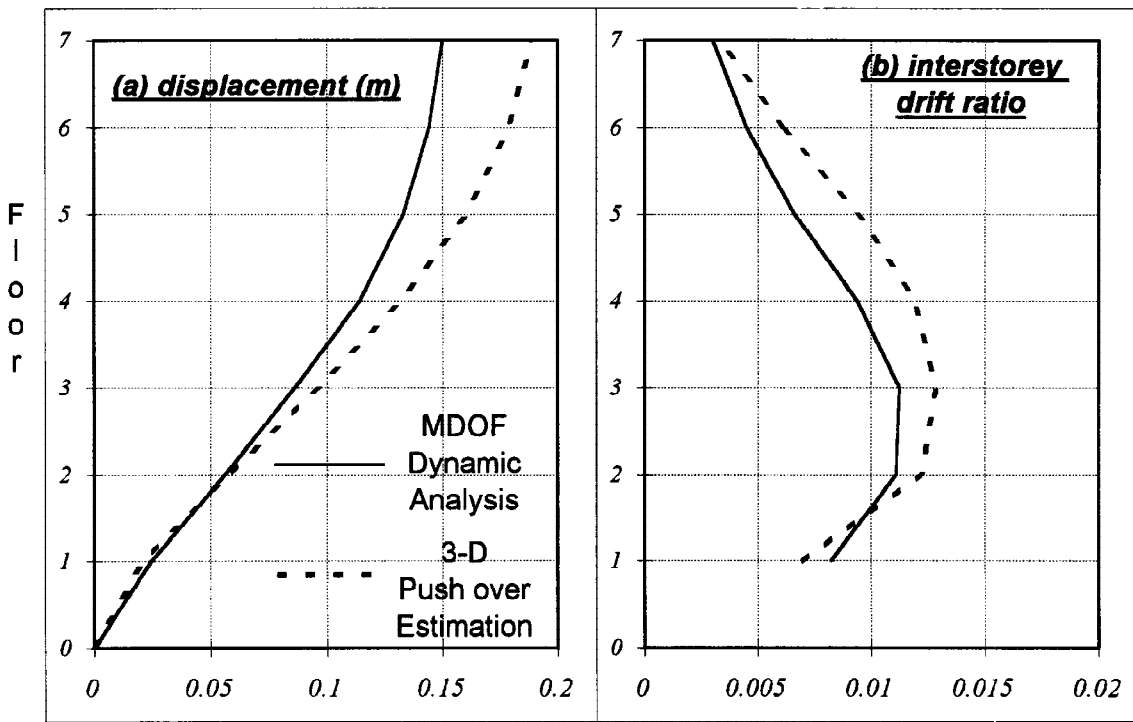


Fig. 10. Maximum displacement and interstorey drift ratio of flexible edge (Whitier EQ record)

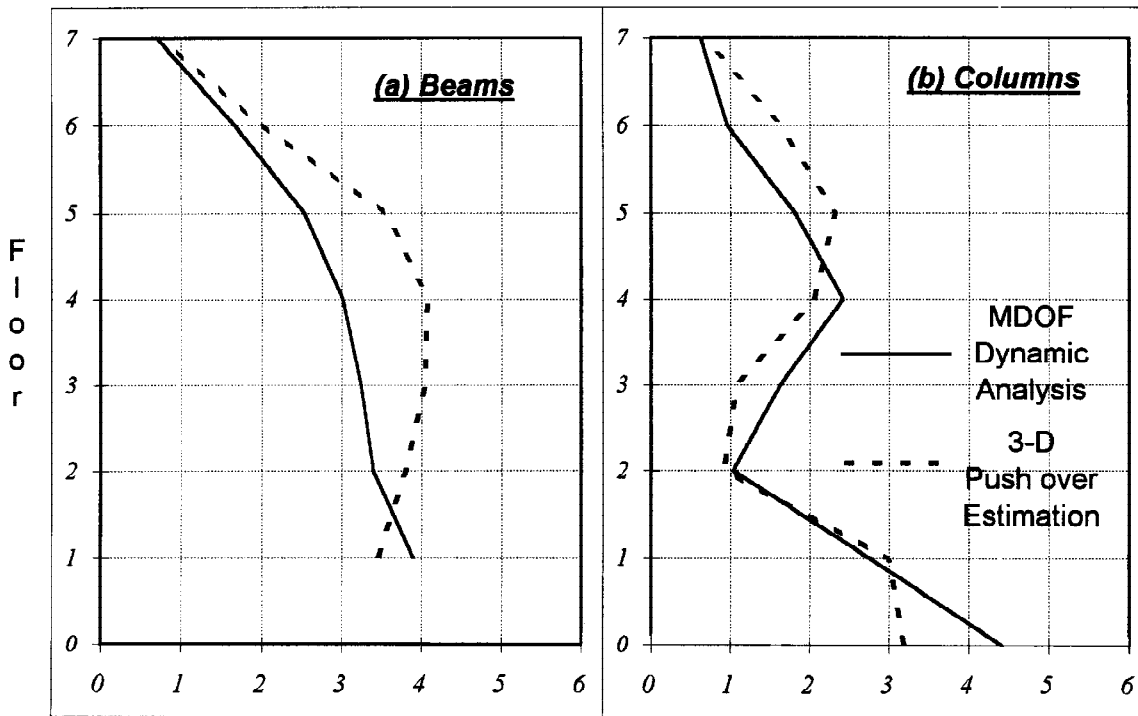


Fig. 11. Maximum ductility demands in beams and columns on Frame 3 (Whitier EQ record)